FEBS Letters

FEBS PRESS science publishing by scientists

RESEARCH ARTICLE

The toxic effects of yeast Ppz1 phosphatase are counteracted by subcellular relocalization mediated by its regulatory subunit Hal3

Marcel Albacar, Diego Velázquez, Antonio Casamayor and Joaquín Ariño

Institut de Biotecnologia i Biomedicina & Departament de Bioquímica i Biologia Molecular, Universitat Autònoma de Barcelona, Cerdanyola del Vallès, Spain

Correspondence
J. Ariño, Institut de Biotecnologia i Biomedicina & Departament de Bioquímica i Biologia Molecular, Universitat Autònoma de Barcelona, 08193, Cerdanyola del Vallès, Spain
Tel: +34 935811315
E-mail: joaquin.arino@uab.es

(Received 29 January 2022, revised 25 February 2022, accepted 1 March 2022)

doi:10.1002/1873-3468.14330

Edited by Ivan Sadowski

Overexpression of *Saccharomyces cerevisiae* protein phosphatase Ppz1 strongly impairs cell growth. Ppz1 is negatively regulated by its subunit Hal3, and Hal3 overexpression fully counteracts the toxic effects derived from high levels of the phosphatase. We show that Ppz1 localizes at the plasma membrane, and that co-expression of Hal3 recruits Ppz1 to internal membranes (mostly vacuolar). This effect is not observed in a catalytically impaired mutant of Ppz1. Disruption of intracellular trafficking by deletion of the ESCRT-0 component *VPS27* abolishes both Hal3-mediated relocalization of Ppz1 and normalization of cell growth, without affecting Ppz1 protein levels. We propose that Hal3 counteracts the toxic effects caused by excess of Ppz1 not only by inhibiting its enzymatic activity but also by recruiting the phosphatase to internal structures.

Keywords: intracellular trafficking; overexpression toxicity; protein phosphatase; yeast

The Ppz protein phosphatases belong to the PP1 family of Ser/Thr phosphatases and are represented in *S. cerevisiae* by two paralogs, Ppz1 and Ppz2 [1,2]. These proteins are characterized by a conserved catalytic C-terminal region (~ 340 residues, about 60% identical to the *bona fide S. cerevisiae* PP1 catalytic subunit Glc7) that is preceded by a much more divergent ~ 350 residues long N-terminal region [3,4]. Ppz1 is the most functionally relevant enzyme, and it is involved in the maintenance of monovalent cation homeostasis. This occurs by regulating two different processes, the repression of the expression of the Ena1 Na^+, K^+-ATPase, crucial in the response to salt stress [5,6], and the inhibition of potassium uptake through the K^+ high-affinity Trk1 and Trk2 transporters [7,8]. The increased K^+ uptake observed in *ppz1* cells, which would lead to increased turgor pressure, was proposed to explain the sensitivity of this strain to cell wall stress situations [4,5,9,10]. Ppz1 appears also involved in translation initiation [11], in the regulation of ubiquitin turnover [12], and the dephosphorylation of the ubiquitin ligase adaptor Art1 [13].

Early reports demonstrated that even moderately higher than normal levels of Ppz1 cause a dramatic cell growth arrest [9,14]. In fact, a more recent genome-wide study showed that Ppz1 could be the most toxic protein in *S. cerevisiae* [15]. Current evidence indicates that such toxicity derives from alteration of multiple targets affecting intracellular signalling [16,17], and the abnormal activation of the Nha1 Na^+,K^+/H^+ antiporter [18]. Remarkably, while the phosphatase activity of Ppz1 is required for toxicity [16], the N-terminal half of Ppz1 also contributes to this effect [19].

Abbreviations

EGFP, enhanced green fluorescent protein; ESCRT, endosomal sorting complex required for transport; PP1, protein phosphatase 1; Ppz1, serine/threonine protein phosphatase Z1.

Ppz1 is controlled by two regulatory subunits, Hal3 and Vhs3 (Hal3 being the major regulator *in vivo*), which play a regulatory role by interacting with the catalytic C-terminal domain of the phosphatase and inhibiting its activity [9,20–23]. Notably, in *S. cerevisiae* and related fungi, Hal3 and Vhs3 are moonlighting proteins that also play a role in the biosynthesis of coenzyme A. This occurs by interaction with Cab3, a structurally related protein, to form an atypical heterotrimeric phosphopantothenoylcysteine decarboxylase (PPCDC) enzyme [24]. It has been proposed that Hal3 has a higher propensity than Vhs3 to be released as a monomer, thus being more able to interact with Ppz1 [22].

In concordance with the inhibitory role of Hal3 on Ppz1 function, episomal expression of Hal3 eliminates the growth defect observed in cells expressing *PPZ1* both from its own promoter in a multicopy plasmid [9] and from the powerful *GAL1* promoter [16]. In spite of some discrepancies among databases constructed from large-scale screening experiments (ref. [25] and https://yplp.yeastgenome.org/), it is generally accepted that Ppz1 can be detected mainly at the cell periphery, likely attached to the plasma membrane because of its conserved myristoylated Gly2 [7,13,14,19,26]. With the aim to better understand the mechanism by which Hal3 could neutralize Ppz1 toxicity, we overexpressed fluorescently tagged versions of Ppz1 and Hal3. To our surprise, we found that Hal3 was able to recruit Ppz1 to internal membranes (mostly vacuolar) and that disruption of this intracellular trafficking abolished Hal3-mediated normalization of cell growth. These results suggest that, in addition to the inhibition of its enzymatic activity, removal of Ppz1 from the plasma membrane contributes to counteract the toxic effects caused by an excess of the phosphatase.

Materials and methods

Yeast strain growth and media

Saccharomyces cerevisiae cells were grown at 28 °C in YPD (1% yeast extract, 2% peptone and 2% dextrose) or synthetic medium with the appropriate drop-out mix of amino acids for plasmid selection when needed. The synthetic medium is composed of 0.17% yeast nitrogen base (YNB) without ammonium sulfate or amino acids, 0.5% ammonium sulfate, 2% glucose and 0.13% drop-out mix [27]. To culture yeast cells carrying constructs under a *GAL1-10* promoter, glucose was replaced by 2% raffinose. For growing yeast cells to be used in assays involving fluorescence detection, media were prepared sterilizing the corresponding carbon source separately in order to reduce background signal.

Growth tests in drops were done as in [16]. For growth assays in liquid medium, cultures were grown overnight to saturation. Dilutions were made to the indicated OD_{600} in fresh medium and distributed by triplicate in honeycomb plates (Thermo Fisher, Waltham, MA, USA). A Bioscreen C apparatus (Thermo Fisher) was used to monitor cell growth at 28 °C by reading the OD_{600} every 30 min for 2 to 3 days. Plates were shaken at the maximum amplitude setting for 7 min before each measure.

DNA techniques, strains and plasmid constructions

Escherichia coli DH5α cells were used as plasmid DNA host and were grown in LB medium supplemented with 50-$\mu g \cdot mL^{-1}$ ampicillin (when required), at 37 °C. Transformations of *E. coli* and standard recombinant DNA techniques were performed as described [28]. *S. cerevisiae* cells were transformed by the lithium acetate method [29].

Strain MAC003 (*GAL1:PPZ1-EGFP*) was constructed by transforming strain ZCZ01 with the cassette GFP-HIS3MX6, following the methodology described in [30], with the pYM28 vector and oligonucleotides S3 Ppz1 Ct Fluo Fw and S2 Ppz1 Ct Fluo Rev. The strain DBY746 *vps27* was made by transformation of wild-type DBY746 cells with a 1.6 kbp *vps27::kanMX4* fragment, amplified with oligonucleotides VPS27-F and VPS27-R, from the BY4741 deletant (EUROSCARF collection). The correct insertion of cassettes was assessed by colony PCR. Strains used in this work are described in Table 1.

Generation of C-terminally GFP-tagged versions of Ppz1 and $Ppz1^{G2A}$ expressed from plasmid YEplac195 (2-micron, *URA3*) was described in [19]. The equivalent construct expressing the catalytically impaired R451L Ppz1 version was made by replacing the PacI and Kpn2I fragment of YEp195 Ppz1-GFP with the equivalent one from the pCM189 Ppz1-R451L construct (laboratory stock). The YEp195 Ppz1-mCherry vector was obtained by PCR amplification of the PPZ1-mCherry fragment from strain

Table 1. Yeast strains used in this work.

Strain Name	Genotype	Origin / Reference
DBY746	*MATα ura3-52 leu2-3,112 his3-1 trp1-239*	D. Botstein
DBY746 *vps27*	DBY746 *vps27::kanMX4*	This work
DVS004	DBY746 *HAL3-GFP*	This work
DVS007	DBY746 *PPZ1-mCherry*	This work
DVS008	DBY746 *HAL3-mCherry*	This work
BY4741	*MATa his3Δ1 leu2Δ0 met15Δ0 ura3Δ0*	[43]
ZCZ01	BY4741 *pGAL1-10:PPZ1*	[16]
MAC003	ZCZ01 *pGAL1-10:PPZ1-EGFP: HIS3MX6*	This work

DVS007 using the oligonucleotides PPZ1_Fw_-470_KpnI and EGFP_mCherry_Rv_HindIII. This fragment was subcloned in YEp195 by restriction (KpnI and HindIII) and subsequent ligation. Strain DVS007, which carries a C-terminally mCherry-tagged version of *PPZ1*, was made by transformation of the wild-type strain DBY746 with a PPZ1-mCherry-kanMX4 cassette obtained by PCR amplification from the pFA6a-mCherry-kanMX4 plasmid using S3_Ppz1_Ct_Fluo_Fw and S2_Ppz1_Ct_Fluo_Rev primers.

Plasmid YEplac181-Hal3 was reported in [6]. YEp181 Hal3-GFP and YEp181 Hal3-mCherry were prepared by PCR amplification from strain DVS004 (*HAL3-GFP*) or DVS008 (*HAL3-mCherry*) genomic DNA, respectively, using oligonucleotides HAL3_Fw_-500_EcoRI and EGFP_mCherry_Rv_HindIII. The fragment was subcloned in YEp181 by restriction with EcoRI and HindIII. Strain DVS004 and DVS008 were made by the transformation of strain DBY746 with a cassette amplified from plasmid pYM28 [30] or pFA6a-mCherry-kanMX6 [31], respectively, and primers S3_Hal3_Ct_Fluo_Fw and S2_Hal3_Ct_Fluo_Rev. Oligonucleotides used in this work are described in Table S1.

Plasmid pRS315 mCherry-HDEL, a centromeric vector (*LEU2* marker) containing the ER localization signal tagged with mCherry, was a gift of Dr. Oriol Gallego (Pompeu Fabra University, Barcelona).

Microscopy techniques

Fluorescence microscopy observation of living cells was performed as follows. Cells were grown overnight to saturation in synthetic media, prepared as described in the Yeast Strains and Media section. At this point, cells were diluted to OD_{600} = 0.2 in fresh media and growth was resumed at 28 °C until OD_{600} = 0.6 was reached. One-mL dilutions at OD_{600} = 0.12 were then prepared, and 300 µL loaded to a well of a µ-Slide 8 Well (Ibidi), previously coated with 10 µL Concanavalin A (1 mg·mL^{-1}) (Merck, Darmstadt, Germany). The µ-Slide 8 Well was incubated for 30 min at 28 °C to let cells settle to the bottom of the wells.

For the MAC003 strain, the medium contained 2% raffinose instead of glucose. When cells reached OD_{600} = 0.6, galactose was added to the culture at a final concentration of 2%, to induce Ppz1 overexpression.

Vacuolar staining with FM4-64 was done in exponentially growing cells (OD_{600} = 0.6) essentially as in [32] except that synthetic medium was used instead of YPD. The incubation time with FM4-64 was 30 min. Cells were then deposited in a µ-Slide 8 Well and observed under the microscope with a Texas Red filter. Unless otherwise stated, pictures were taken using a Nikon Eclipse TE2000-E fluorescence microscope.

Immunoblot detection of Ppz1 and Hal3

Yeast protein extracts were prepared as follows. Cultures were grown until OD_{600} = 0.8. Cells were collected by centrifugation (5 min at 1000 × ***g***), supernatants were discarded and pellets were resuspended in 100 µL of Lysis Buffer (50 mM Tris-HCl pH 7.5, 150-mM NaCl, 10% Glycerol, 0.1% Triton X-100) supplemented with 1-mM fresh DTT and EDTA-free Protease Inhibitor Cocktail (Roche). Cell lysis was performed by adding 125 µL of Zirconia 0.5-mm beads (BioSpec, Bartlesville, OK, USA) and vigorously shaking the samples in a FastPrep (MP Biomedicals) at 5.5 m·s^{-1} for 45 s (3 cycles, cooling the tubes on ice for 2 min between repeats). Twenty-five microlitres of Lysis Buffer were added to the samples, and these were centrifuged for 10 min at 650 × ***g*** at 4 °C. After this, supernatants were recovered, and the total protein was quantified by the Bradford method (Sigma-Aldrich).

Protein extracts containing 40 µg of protein were mixed with 4× SDS/PAGE loading buffer (200 mM Tris–HCl (pH 6.8), 8% (w/v) sodium dodecyl sulfate (SDS), 0.4% (w/v) bromophenol blue, 40% (v/v) glycerol, 20% (v/v) β-mercaptoethanol), so that the final concentration was 1×, heated at 95 °C for 5 min and resolved by SDS/PAGE. Proteins were transferred to a polyvinylidene difluoride (PVDF) membrane (Immobilon-P, Millipore, Burlington, MA, USA) by semi-dry transfer using a TE77XP apparatus (Hoefer, Holliston, MA, USA). Ppz1 was detected using an anti-GST-Ppz1 antiserum [3], at a 1 : 250 dilution in TBST (Tris-buffered saline plus 0.1% Tween 20) supplemented with 5% fat-free powdered milk. Hal3 was detected using a polyclonal anti-Hal3 antibody [33] at a 1 : 500 dilution as above. In both cases, a 1 : 20 000 dilution of secondary anti-rabbit IgG-horseradish peroxidase antibodies (GE Healthcare, Chicago, IL, USA) was employed. For detection of the GFP tag, a primary anti-GFP monoclonal antibody (Invitrogen, #9F9.F9, 1 : 1000 dilution) followed by secondary anti-mouse IgG-horseradish peroxidase antibody [(GE Healthcare), 1 : 10000 dilution] was used.

Results

Expression of Hal3 from a multicopy plasmid alters the subcellular localization of the native version of Ppz1

As documented in the Introduction section, previous reports described that Ppz1 was mostly associated with the peripheral membrane. The ability to associate with membranes was attributed to the myristoylable Gly at position 2 [14], and recent work demonstrated that mutation of Gly2 to Ala results in disappearance of the phosphatase from the cell's periphery and uniform distribution inside the cell [13,19]. We tested here whether the phosphatase function of Ppz1 was relevant for its subcellular localization by constructing a GFP-tagged version of Ppz1-R451L, a nearly inactive version of the phosphatase [14] whose overexpression barely affects cell growth [16].

As seen in Fig. 1A, in our experimental setting (Ppz1 expressed from its own promoter in a multicopy plasmid), the native version of the phosphatase mostly localizes at the peripheral membrane in a somewhat punctuated pattern, with minor presence in some internal structures. The inactive version shares the peripheric localization of the native Ppz1-GFP version, although its presence in internal structures appears more accentuated. As previously described, when Gly2 is changed to Ala, Ppz1 no longer localizes in peripheral or internal membranes, but it becomes dispersed within the cell. These results indicate that the activity of the phosphatase is not a crucial requirement for its subcellular localization and confirms the relevance of Gly2 as a key structural requirement for Ppz1 intracellular distribution. We then tested whether co-overexpression of Hal3 had any effect on Ppz1 intracellular localization. Remarkably, as shown in Fig. 1B, the presence of Hal3 resulted in substantial removal of Ppz1 from the cell periphery and in its accumulation in conspicuous intracellular structures, which was detectable in 53.3% of the cells monitored. This behaviour was much less evident (13.4%) in the Ppz1-R451L version, whereas co-expression of Hal3 did not alter at all the diffuse distribution of the G2A variant. In this case, co-expression of Hal3 led to higher levels of Ppz1-GFP as it can be deduced from the brighter image, and this was subsequently confirmed by immunoblot analysis (data not shown).

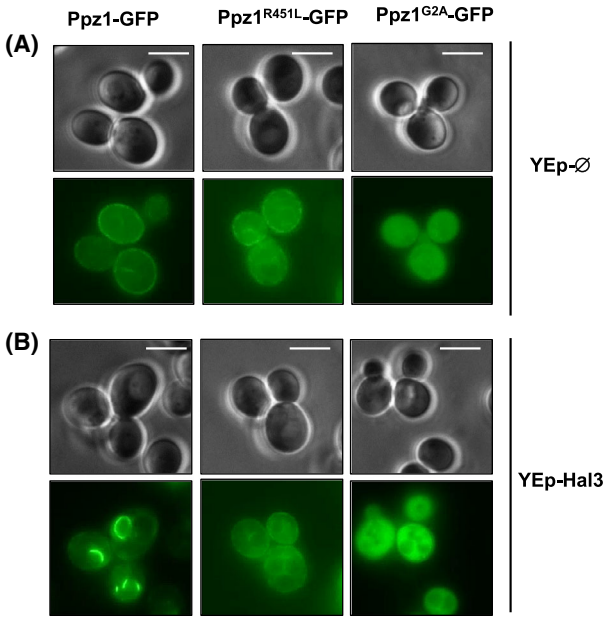

Fig. 1. Expression of Hal3 from a multicopy plasmid alters the subcellular localization of the native version of Ppz1. (A) DBY746 cells carrying the indicated combinations of plasmids were treated as described in Materials and Methods and observed at the fluorescence microscope. The GFP signal was captured with a FITC filter. Excitation was performed during 3000 (panel A) or 1500 ms (panel B). YEp-ø denotes the empty YEplac181 vector. Bars (5 μm) are included for reference. The number of cells examined ranged from 127 to 341.

Overexpressed Ppz1 and Hal3 colocalize in internal, mostly vacuolar membranes

The surprising behaviour of Ppz1 in cells overexpressing Hal3 prompted us to investigate the subcellular localization of this regulatory subunit. To this end, a GFP-tagged version of Hal3 was constructed and its localization monitored in control cells or cells overexpressing Ppz1. As shown in Fig. 2, in the absence of Ppz1 overexpression, Hal3 was evenly distributed in the cytosol. However, when Ppz1 was overexpressed, although part of the Hal3 signal remained diffusely distributed in the cytosol, a significant signal was also detected in structures whose shape was reminiscent to those observed for GFP-tagged Ppz1 (32.8% of monitored cells). This result suggested that Hal3 might actually escort Ppz1 to this particular subcellular location. To test this possibility, new constructs expressing mCherry-tagged versions of Ppz1 and Hal3 were prepared and colocalization experiments carried out. As observed in Fig. 3, the distribution patterns of the phosphatase and its regulatory subunit were largely overlapping (> 95% of cells with signal for both dyes), suggesting a concurrence of both proteins at the same intracellular structures. The shape and number of the observed structures were compatible with the membranes of certain organelles such as vacuoles or

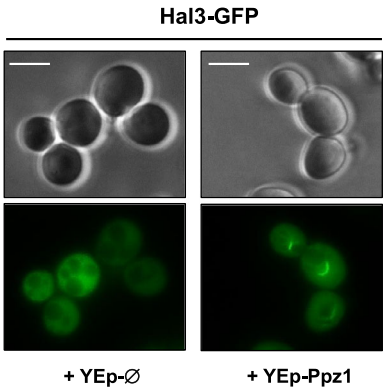

Fig. 2. Hal3-GFP is cytosolic but can be detected in internal structures when Ppz1 is expressed from a multicopy plasmid. DBY746 cells were transformed with a multicopy Hal3-GFP vector plus an empty YEp vector (YEp-ø) or the same vector carrying *PPZ1*, as indicated. The GFP signal was captured during 1000 ms. At least 200 cells were examined.

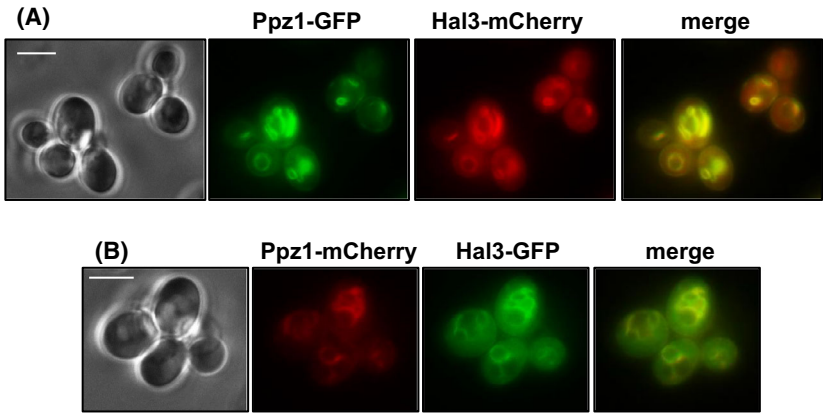

Fig. 3. Ppz1 and Hal3 colocalize in internal structures *in vivo*. DBY746 carrying the following combination of plasmids: (A) Ppz1-GFP + Hal3-mCherry and (B) Ppz1-mCherry + Hal3-GFP were treated as described in Materials and Methods. GFP and mCherry signal were analyzed using a FITC and a Texas Red filter respectively. Excitation was performed during 1500 ms for GFP and 2000 ms for mCherry. A minimum of 250 cells per condition was monitored.

perinuclear endoplasmic reticulum (ER). To test the possibility of Ppz1 being located at vacuolar membranes, we stained these membranes with the lipophilic dye FM4-64 [34]. As shown in Fig. 4A, substantial colocalization of Ppz1-GFP with structures stained with FM4-64 was observed, and this phenomenon was identified in nearly half (44.2%) of monitored cells. Similarly, Ppz1-GFP was co-expressed with a plasmid carrying mCherry associated with the HDEL sequence, which promotes ER localization [35]. With this tool, we could observe in some instances (10.6% of examined cells after 2 h and 11.7% after 6 h of induction) colocalization of Ppz1-GFP with mCherry-HDEL containing membranes (Fig. 4B). It is worth noting that Ppz1-GFP does not decorate the entire vacuolar or ER membranes, suggesting the existence of preferential localization regions. Therefore, it can be concluded that concomitant overexpression of Ppz1 and Hal3 directs the phosphatase from the plasma membrane to internal membranes (mostly the vacuolar membrane) and that Ppz1 is accompanied by its negative regulatory subunit.

Effect of the presence of Hal3 in the localization of conditionally expressed Ppz1

The experiments presented above involve the co-expression of Ppz1 and Hal3 from their own

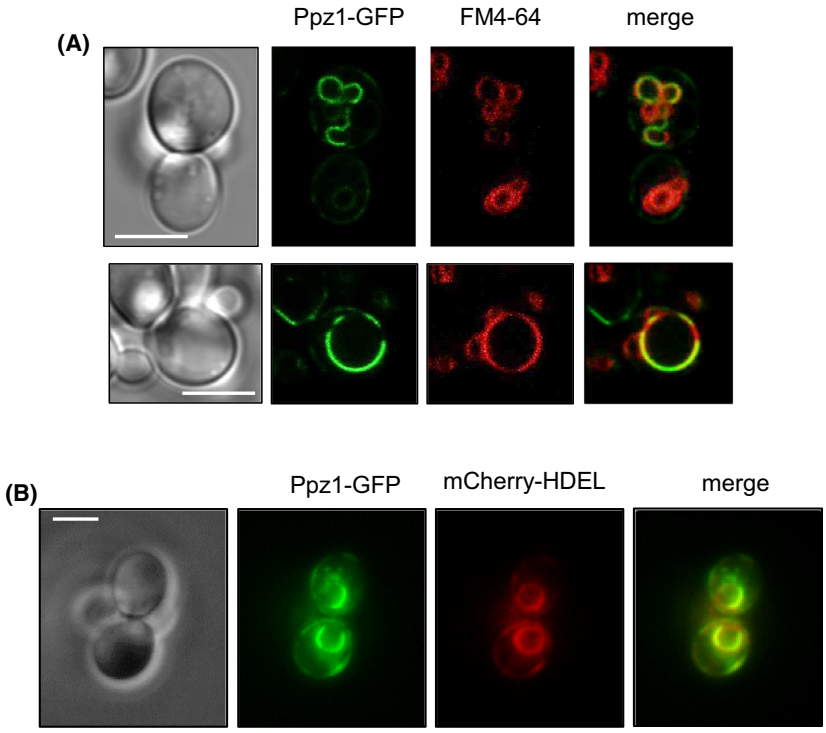

Fig. 4. Ppz1 mainly localizes in vacuolar membranes when cells carry a Hal3 multicopy plasmid and in some cases in the ER. (A) DBY746 cells carrying the plasmids YEp195 Ppz1-GFP and YEp181 Hal3 were treated with FM4-64 as described in Materials and Methods. Cell were then monitored in a confocal microscope (Leica TCS SP5). Two hundred fifty eight cells were analyzed. (B) MAC003 cells transformed with plasmids YEp195 Hal3 and pRS315 mCherry-HDEL and cells observed after 2 h of galactose addition under a Nikon Eclipse TE2000-E fluorescence microscope. A total number of 218 cells were analyzed, and ER localization was observed in 10.6% of the population.

promoters and a multicopy plasmid. It is known that the expression level achieved for Ppz1 in this experimental setting is relatively modest, due to copy number restriction [15]. We wanted to know whether the observed shift of Ppz1 from the plasma membrane to internal membranes could also be observed when Ppz1 was expressed at higher levels from a chromosomal copy and driven by the powerful *GAL1* promoter. To this end, we created strain MAC003, which is equivalent to the previously characterized strain ZCZ01 [16,17], although in this case Ppz1 contains a C-terminal GFP tag. As shown in Fig. S1, the intensity of the toxic effect of GFP-tagged Ppz1 in strain MAC003 is indistinguishable from that of strain ZCZ01. Thus, strain MAC003 became an interesting tool because it allowed following the fate of Ppz1 within the cell during the process of accumulation of the phosphatase. When the level of Ppz1-GFP accumulation in MAC003 cells was monitored by immunoblot (Fig. 5A), we observed that the phosphatase was undetectable prior induction, as expected for *GAL*-driven expression in cells growing on raffinose, and that its level increased with time and remained high at least until 20 h after induction. Microscopic analysis of these cultures (Fig. 5B) showed that, in the absence of Hal3 co-expression, Ppz1-GFP was already detectable (albeit with a relatively weak signal) at the cell periphery after 2 h of induction. The Ppz1 signal increased with time and largely maintained its peripheral distribution. Remarkably, when Hal3 was co-expressed, after 2 h of induction, Ppz1 was already identifiable in internal structures in 16.7% of the cells. The intensity and abundance of these intracellular signals increased after 4 and 6 h of induction (38.7% and 42.5% of cells, respectively), with lesser amounts of Ppz1 observable at the periphery. After 20 h of induction, most Ppz1 was found associated with internal structures (80.1% of cells), and little or no signal was detected at the cell periphery. These results suggests that the presence of Hal3 allows removal of Ppz1 from the plasma membrane as soon as the level of the phosphatase may become dangerous for the cell (see Discussion). It is worth noting that the presence of Ppz1 at these internal

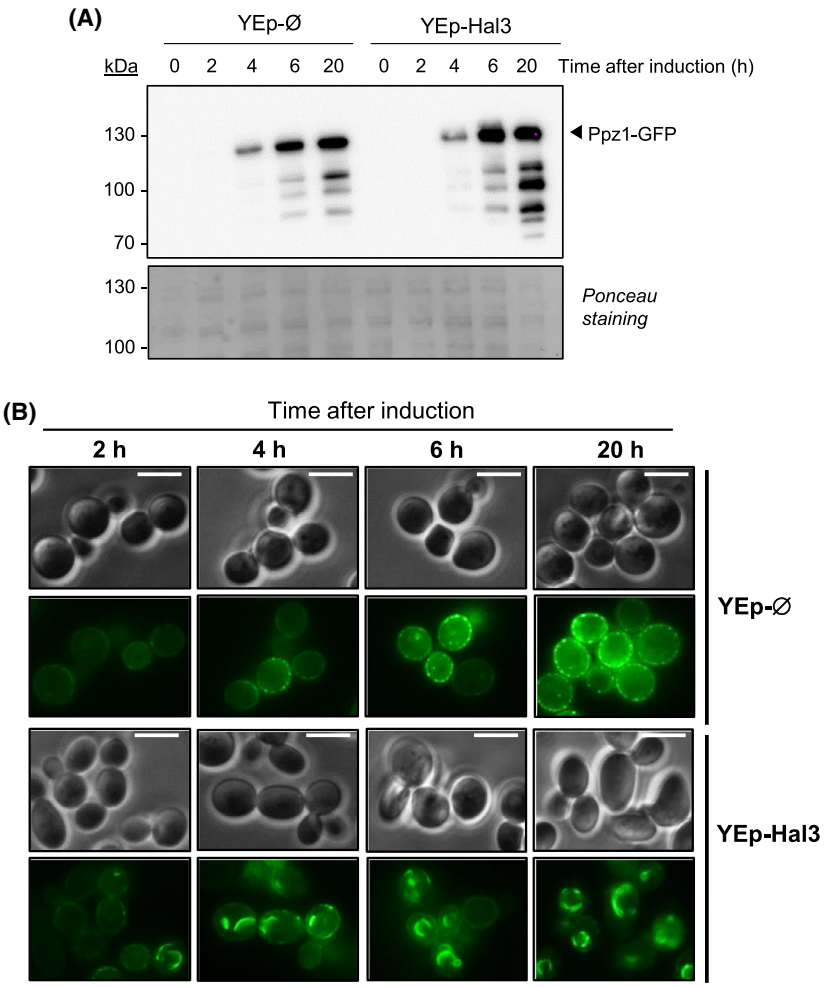

Fig. 5. Time course of Ppz1-GFP expression and localization in the MAC003 strain. MAC003 cells transformed with an empty YEplac195 plasmid (YEp-ø) or with the same vector carrying *HAL3* (YEp-Hal3) were grown until saturation, and cultures were processed for Ppz1 overexpression. (A) Cultures were processed for SDS/PAGE electrophoresis (8% acrylamide gels) and transferred to membranes. Ppz1-GFP was detected by mean of anti-GFP antibodies. No bands below the 70 kDa marker were observed. Ponceau red staining is shown to monitor loading and transfer efficiency. (B) Monitoring of Ppz1-GFP signal in cultures prepared as above at the fluorescence microscope at different times upon induction. The number of cells documented ranged from 144 to 328. Exposition was performed during 3000 ms (YEp-ø) and 1500 ms (YEp-Hal3).

structures is not a transient event, as it is observed even 20 h after induction of the expression.

Mutation of *VPS27* disrupts Ppz1-Hal3 colocalization in internal structures and impairs Hal3-mediated growth improvement

Overexpression of Hal3 from a multicopy plasmid is able to fully eliminate the growth defect of cells overexpressing Ppz1 from its own promoter in high-copy number [9] or from the *GAL1* promoter (reference [16] and Fig. S1). Therefore, we wanted to test whether the ability to normalize cell functions was related to the shift in subcellular localization. To this end, we used a *vps27* deletion mutant, which lacks the Vps27 protein, a component of the Endosomal Sorting Complex Required for Transport (ESCRT) [36]. Wild-type DBY746 and *vps27* cells were transformed with YEp195 Ppz1-GFP plus either YEp181 or YEp181 Hal3. As presented in Fig. 6, co-expression of Ppz1 and Hal3 in the wild-type strain shows Ppz1 associated with the mentioned internal membranes. In contrast, these were rarely seen in the *vps27* background (4.1% of cells), while more Ppz1 could be detected at the cell periphery. In addition, in the *vps27* strain, Hal3 showed a diffuse cytoplasmatic localization, with minimal localization at internal structures when Ppz1 was co-expressed (3.6% of cells). Therefore, the lack of Vps27 disturbs the observed relocalization of Ppz1 and Hal3 when both proteins are co-expressed. Prompted by these results, we monitored growth in wild-type and *vps27* cells overexpressing Ppz1-GFP and in the presence or absence of Hal3 overexpression. As shown in Fig. 7A, the *vps27* mutation by itself did not significantly affect growth of cells carrying the empty plasmids, while expression of Ppz1-GFP from the multicopy plasmid moderately impaired growth of the wild-type strain. It is worth noting that expression of Ppz1 from its own promoter, even from a multicopy plasmid, results in less dramatic effects on growth than when the phosphatase is expressed from the strong *GAL* promoter (compare with Fig. S1). Interestingly, overexpression of Ppz1 in the *vps27* background resulted in a growth defect much more dramatic than that observed in the wild-type strain. In addition, while in the wild-type background overexpression of Hal3 fully counteracted the impact of Ppz1 overexpression, the growth defect was barely attenuated in the case of the *vps27* strain. It is important to note that, as deduced from the immunoblot analysis presented in Fig. 7B, overexpression of Hal3 allows a much higher accumulation of Ppz1, but the levels of Ppz1 and the proportion between the amounts of Ppz1 and Hal3 in wild-type and *vps27* cells are very much alike. This implies that the strongly impaired growth of *vps27* cells expressing Ppz1 is not due to an abnormal

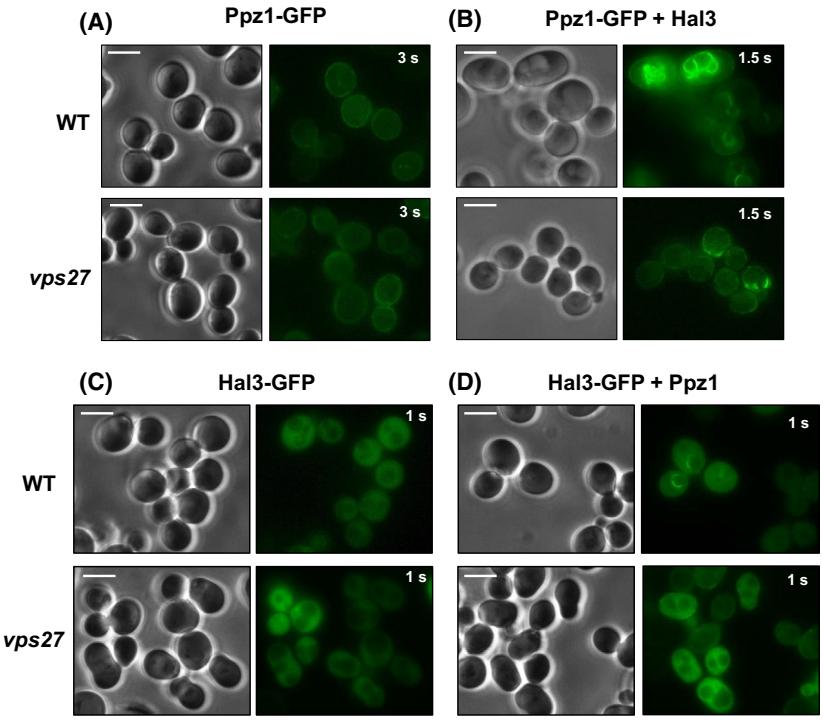

Fig. 6. Mutation of *VPS27* disrupts colocalization of Ppz1 and Hal3 in internal structures. DBY746 (WT) and *vps27* cells carrying the combination (A) Ppz1-GFP + empty vector, (B) Ppz1-GFP + Hal3, (C) empty vector + Hal3-GFP and (D) Ppz1 + Hal3-GFP were grown until saturation in the appropriate selective medium and treated as described in Material and Methods. Pictures are representative of 257 to 343 documented cells. The time of exposure is shown for each image.

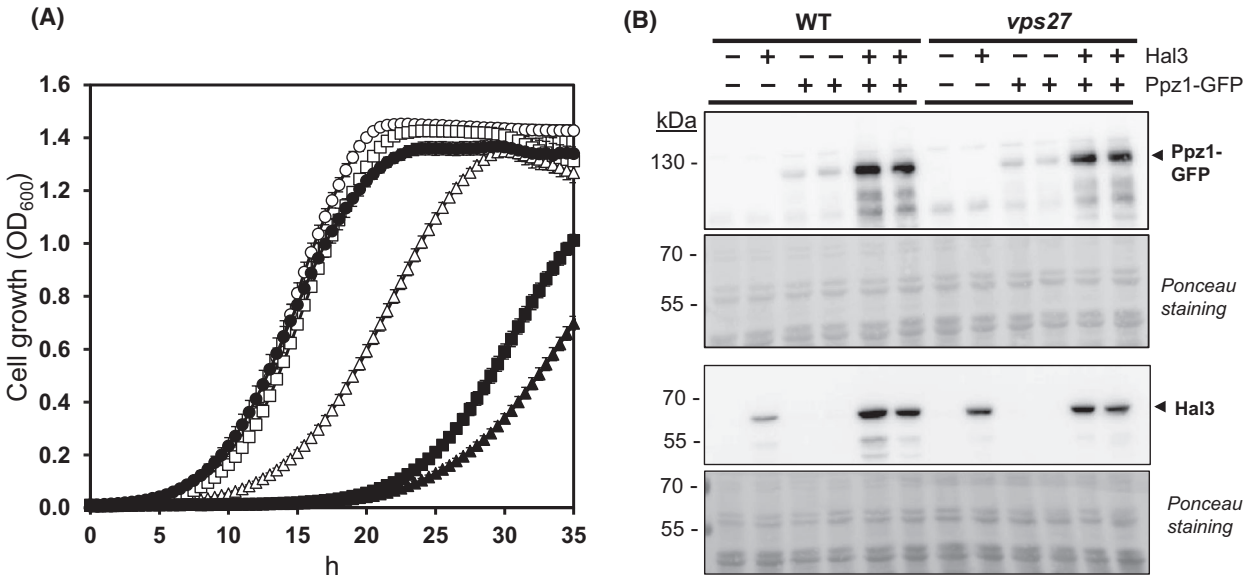

Fig. 7. Mutation of *VPS27* aggravates Ppz1 toxicity and impairs Hal3-mediated growth rate normalization. (A) Wild-type strain DBY746 (WT, empty symbols) and *vps27* (filled symbols) were co-transformed with the empty vectors (circles), Ppz1-GFP plus an empty vector (triangles) or Ppz1-GFP plus the YEp-Hal3 plasmid (squares). Cells were processed for growth determination in liquid culture at an initial OD_{600} of 0.02. Values are the mean ± SEM of 5 to 12 independent cultures. (B) Immunodetection of Ppz1 and Hal3 levels in DBY746 (WT) and *vps27* cells. Whole yeast extracts were prepared as described in Materials and Methods (cultures carrying Ppz1-GFP were grown and assayed in duplicate). Two gels (10% acrylamide) were loaded in parallel; one was processed for anti-Ppz1 detection (upper panel); and the other for anti-Hal3 detection (lower panel). Ponceau red staining is shown to verify loading and transfer efficiency.

accumulation of the phosphatase or to insufficient expression levels of the regulatory subunit. Therefore, these results indicate that the lack of *vps27* clearly worsens the toxic phenotype derived from Ppz1 overexpression and that, in the absence of this essential component of the ESCRT pathway, the presence of Hal3 cannot modify the intracellular localization of Ppz1 nor alleviate the growth defect caused by the excess of phosphatase.

Discussion

We confirm in this work that, upon overexpression, most Ppz1 can be detected at the cell periphery and that the myristoylable Gly2 is a requisite for such peripheral localization. We also demonstrate that, in contrast, the phosphatase function of Ppz1 is not essential for its localization. More importantly, our results indicate that in cells co-expressing Ppz1 and Hal3, most Ppz1 is removed from the cell periphery and recruited in internal membranes. This is not observed for the catalytically impaired Ppz1 version, suggesting that relocalization of Ppz1 is triggered by the excess of Ppz1 activity. Similarly, the $Ppz1^{G2A}$ version remains fully cytosolic when Hal3 is co-expressed, suggesting that myristoylation of Gly2 would be necessary for the relocalization process.

We observed that, whereas Hal3 accompanied Ppz1 to these internal structures, significant amounts of this regulatory subunit were still detected at the cytosol. This could be explained by Hal3's moonlighting function in CoA biosynthesis : a portion of Hal3 molecules would remain cytosolic as part of the PPCDC complex [24,37]. Using strain MAC003, we also observe (Fig. 5) that Ppz1 is recruited to internal structures shortly after its expression is induced (2 h). It should be noted that our recent work with the equivalent strain ZCZ01 demonstrated that 2 h of induction is sufficient to provoke dramatic changes in the transcriptome and phosphoproteome of the cell, and a significant arrest in cell proliferation [16–18]. Since co-expression of Hal3 fully normalizes cell growth, it could be assumed that the toxic effects of Ppz1 are neutralized as soon as they appear by means of Hal3-mediated relocalization of the phosphatase.

Because most known targets for Ppz1, such as Trk1/Trk2 and Nha1 (and perhaps Pma1), are located at the plasma membrane, one might assume that removal of Ppz1 from the cell periphery should be sufficient for

counteracting toxicity. However, the observation that, when expressed from plasmid pCM190 (a *tetO*-regulatable vector), mutation of Gly2 to Ala leads only to a slight attenuation of toxicity [19], indicates that very relevant targets for Ppz1 toxicity are not located at the plasma membrane. Among such targets could be diverse cytosolic protein kinases (i.e. Rck2, Tda1, Npr1, Hog1 or Snf1) whose phosphorylation state (and likely activation state) was found significantly altered upon short-time induction of Ppz1 expression [17]. Therefore, one could assume that relocalization of Ppz1 to internal membranes would be a strategy not only to remove Ppz1 from the plasma membrane, but also to avoid excessive amounts of cytosolic phosphatase. Because, as far as we know, Ppz1 has not been identified by proteomic analysis in vacuolar membranes of cells grown under standard conditions [25], it could be postulated that relocalization of Ppz1 would be, rather than an ordinary regulatory mechanism, an exceptional safeguard instrument against the toxic effects of Ppz1. This concept fits well with the observation that the inactive version of the phosphatase ($Ppz1^{R451L}$), which is expressed at higher levels than native Ppz1 but has virtually no effect on cell growth [16], is not internalized by co-expression of Hal3 (Fig. 1). It is unknown what would be the trigger for the association of Ppz1 and Hal3 leading to the accumulation of both proteins at internal membranes. However, we showed very recently that cells overexpressing Ppz1 suffer a drop in internal pH, likely due to the combination of an hyperactivation of Nha1 and the inhibition of the Pma1 proton pump [18]. It has been proposed that the interaction between Ppz1 and Hal3 could be modulated by pH, in a way that acidification would increase Ppz1-Hal3 interaction [7]. Therefore, a plausible scenario would be that the abnormal intracellular acidification would lead to an increased interaction between Hal3 and Ppz1 that would firstly result in direct inhibition of the Ppz1 activity and then in the sequestering of the phosphatase away from its targets.

The notion that Hal3-mediated relocalization of Ppz1 to internal membranes is crucial for toxicity safeguard is reinforced by the observation that mutation of *VPS27* eliminates Ppz1 relocalization, worsens the cell growth defect of cells overexpressing Ppz1 and largely abolishes the beneficial effect of co-expression of Hal3. We have no reason to believe that elimination of Vps27 might affect the ability of Hal3 to directly interact with Ppz1 and to inhibit its phosphatase activity. Therefore, it must be assumed that the inhibition of Ppz1 activity could be necessary but not sufficient to counteract Ppz1-mediated toxicity. Together with Hse1, Vps27 composes the ESCRT-0 complex, which is the first and necessary step for progression in the ESCRT pathway. This conserved pathway is involved in diverse cellular functions, such as eukaryotic cell abscission, exosome secretion, or macroautophagy and microautophagy, but it has a recognized role in trafficking of membrane proteins to vacuole for degradation [36,38,39]. Our results clearly indicate that the removal of Ppz1 from the plasma membrane requires the ESCRT pathway. However, the current evidence argues against the excess of Ppz1 being directed to the vacuole for degradation because (a) even after a long period of Ppz1 overexpression, the phosphatase is mainly detected in the vacuolar membrane but very rarely in the vacuolar lumen (Fig. 5) and (b) co-expression of Hal3 does not lead to a decrease in the amount of Ppz1, but instead, it allows for the accumulation of the phosphatase [see [16] and Fig. 5A and 7B]. It could be speculated that Ppz1 may be trapped at the vacuolar (and ER) membrane by its N-myristoylated N-terminus. There are some examples of yeast proteins that translocate to the vacuolar membrane as part of their normal function. For instance, *Saccharomyces cerevisiae* Sch9 (a member of the AGC family of protein kinases) displays a dynamic localization, shuttling from cytosol to the vacuolar membrane where it could be phosphorylated and activated by the TORC1 complex leading to specific modulation of the Sch9 branch of TORC1 signalling [40,41]. Another example could be the PpAtg9 protein from *Pichia pastoris*, which localizes in structures near the plasma membrane during methanol growth and, on glucose-induced macropexophagy, it translocates to perivacuolar structures [42]. At this point, it is not clear why Ppz1 is maintained in these internal structures and not directed to degradation, although a possibility could be the recycling of Ppz1 when its levels decrease below the toxic threshold.

Acknowledgements

The technical assistance of Montserrat Robledo is acknowledged. We thank Oriol Gallego (Pompeu Fabra University, Barcelona) for plasmid pRS315 mCherry-HDEL, Ivana Malcova (Institute of Microbiology, CAS, Hungary) for plasmid pFA6a-mCherry-kanMX6 and Cesar Roncero (Universidad de Salamanca, Spain) for inspiring comments on the use of the *vps27* mutant. This research was funded by grant BFU2017-82574-P to JA and AC from the Ministerio de Economía, Industria y Competitividad (Spain). MA and DV were recipient of PhD fellowships from the PIF UAB program (Spain).

Author contributions

AC and JA conceived and supervised the study; MA carried out most of the experiments; DV provided new tools and reagents; MA, AC and JA analysed data; JA wrote the manuscript and all authors made manuscript revisions.

Data accessibility

The data that support the findings of this study are available in Figs. 1 to 7 and the supplementary material of this article (Table S1 and Fig. S1). Additional data, such as sets of micrographs for specific experiments, are available from the corresponding author [Joaquin.Arino@uab.es] upon reasonable request.

References

1 Ariño J, Velázquez D, Casamayor A. Ser/Thr protein phosphatases in fungi: Structure, regulation and function. *Microb Cell*. 2019;**6**:217–56.
2 Offley SR, Schmidt MC. Protein phosphatases of *Saccharomyces cerevisiae*. *Curr Genet*. 2019;**65**:41–55.
3 Posas F, Casamayor A, Morral N, Ariño J. Molecular cloning and analysis of a yeast protein phosphatase with an unusual amino-terminal region. *J Biol Chem*. 1992;**267**:11734–40.
4 Lee KS, Hines LK, Levin DE. A pair of functionally redundant yeast genes (PPZ1 and PPZ2) encoding type 1-related protein phosphatases function within the PKC1-mediated pathway. *Mol Cell Biol*. 1993;**13**:5843–53.
5 Posas F, Camps M, Ariño J. The PPZ protein phosphatases are important determinants of salt tolerance in yeast cells. *J Biol Chem*. 1995;**270**:13036–41.
6 Ruiz A, Yenush L, Ariño J. Regulation of ENA1 Na^+-ATPase gene expression by the Ppz1 protein phosphatase is mediated by the calcineurin pathway. *Eukaryot Cell*. 2003;**2**(5):937–948.
7 Yenush L, Merchan S, Holmes J, Serrano R. pH-Responsive, Posttranslational Regulation of the Trk1 Potassium Transporter by the Type 1-Related Ppz1 Phosphatase. *Mol Cell Biol*. 2005;**25**:8683–92.
8 Yenush L, Mulet JM, Ariño J, Serrano R. The Ppz protein phosphatases are key regulators of K^+ and pH homeostasis: implications for salt tolerance, cell wall integrity and cell cycle progression. *EMBO J*. 2002;**21**:920–9.
9 De Nadal E, Clotet J, Posas F, Serrano R, Gomez N, Ariño J. The yeast halotolerance determinant Hal3p is an inhibitory subunit of the Ppz1p Ser/Thr protein phosphatase. *Proc Natl Acad Sci USA*. 1998;**95**:7357–62.
10 Merchan S, Bernal D, Serrano R, Yenush L. Response of the *Saccharomyces cerevisiae* Mpk1 mitogen-activated protein kinase pathway to increases in internal turgor pressure caused by loss of Ppz protein phosphatases. *Eukaryot Cell*. 2004;**3**:100–7.
11 De Nadal E, Fadden RPP, Ruiz A, Haystead T, Ariño J. A role for the Ppz Ser/Thr protein phosphatases in the regulation of translation elongation factor 1Balpha. *J Biol Chem*. 2001;**276**:14829–34.
12 Lee S, Tumolo JM, Ehlinger AC, Jernigan KK, Qualls-Histed SJ, Hsu P-C, et al. Ubiquitin turnover and endocytic trafficking in yeast are regulated by Ser57 phosphorylation of ubiquitin. *Elife*. 2017;**6**:76.
13 Lee S, Ho H-C, Tumolo JM, Hsu P-C, MacGurn JA. Methionine triggers Ppz-mediated dephosphorylation of Art1 to promote cargo-specific endocytosis. *J Cell Biol*. 2019;**218**:977–92.
14 Clotet J, Posas F, De Nadal E, Arino J. The NH2-terminal extension of protein phosphatase PPZ1 has an essential functional role. *J Biol Chem*. 1996;**271**:26349–55.
15 Makanae K, Kintaka R, Makino T, Kitano H, Moriya H. Identification of dosage-sensitive genes in *Saccharomyces cerevisiae* using the genetic tug-of-war method. *Genome Res*. 2013;**23**:300–11.
16 Calafí C, López-Malo M, Velázquez D, Zhang C, Fernández-Fernández J, Rodríguez-Galán O, et al. Overexpression of budding yeast protein phosphatase Ppz1 impairs translation. *Biochim Biophys Acta Mol Cell Res*. 2020;**1867**:118727.
17 Velázquez D, Albacar M, Zhang C, Calafí C, López-Malo M, Torres-Torronteras J, et al. Yeast Ppz1 protein phosphatase toxicity involves the alteration of multiple cellular targets. *Sci Rep*. 2020;**10**:15613.
18 Albacar M, Sacka L, Calafí C, Velázquez D, Casamayor A, Ariño J, et al. The Toxic Effects of Ppz1 Overexpression Involve Nha1-Mediated Deregulation of K^+ and H^+ Homeostasis. *J Fungi (Basel, Switzerland)*. 2021;**7**:1010.
19 Calafí C, López-Malo M, Albacar M, Casamayor A, Ariño J. The N-terminal region of yeast protein phosphatase Ppz1 is a determinant for its toxicity. *Int J Mol Sci*. 2020;**21**:1–16.
20 Muñoz I, Simón E, Casals N, Clotet J, Ariño J. Identification of multicopy suppressors of cell cycle arrest at the G1 - S transition in *Saccharomyces cerevisiae*. *Yeast*. 2003;**20**:157–69.
21 Ruiz A, Muñoz I, Serrano R, Gonzalez A, Simon E, Arino J. Functional characterization of the *Saccharomyces cerevisiae VHS3* gene: a regulatory subunit of the Ppz1 protein phosphatase with novel, phosphatase-unrelated functions. *J Biol Chem*. 2004;**279**:34421–30.
22 Abrie JA, Molero C, Ariño J, Strauss E. Complex stability and dynamic subunit interchange modulates the disparate activities of the yeast moonlighting proteins Hal3 and Vhs3. *Sci Rep*. 2015;**5**:15774.

23 Abrie JAA, González A, Strauss E, Ariño J. Functional mapping of the disparate activities of the yeast moonlighting protein Hal3. *Biochem J*. 2012;**442**:357–68.
24 Ruiz A, Gonzalez A, Munoz I, Serrano R, Abrie JA, Strauss E, et al. Moonlighting proteins Hal3 and Vhs3 form a heteromeric PPCDC with Ykl088w in yeast CoA biosynthesis. *Nat Chem Biol*. 2009;**5**:920–8.
25 Wiederhold E, Veenhoff LM, Poolman B, Slotboom DJ. Proteomics of *Saccharomyces cerevisiae* Organelles. *Mol Cell Proteomics*. 2010;**9**:431–45.
26 Venturi GM, Bloecher T, Williams-Hart T, Tatchell K. Genetic interactions between *GLC7*, *PPZ1* and *PPZ2* in Saccharomyces cerevisiae. *Genetics*. 2000;**155**:69–83.
27 Adams A, Gottschling DE, Kaiser CA, Stearns T. Methods in yeast genetics : a Cold Spring Harbor Laboratory course manual Cold. Suffolk County, NY, USA: Spring Harbor Laboratory Press. 1998.
28 Sambrook J, Russell DW. Molecular Cloning: A Laboratory Manual. Cold Spring Harbor, NY: Cold Spring Harbor Laboratory Press; 2001.
29 Ito H, Fukuda Y, Murata K, Kimura A. Transformation of intact yeast cells treated with alkali cations. *J Bacteriol*. 1983;**153**:163–8.
30 Janke C, Magiera MM, Rathfelder N, Taxis C, Reber S, Maekawa H, et al. A versatile toolbox for PCR-based tagging of yeast genes: New fluorescent proteins, more markers and promoter substitution cassettes. *Yeast*. 2004;**21**:947–62.
31 Malcova I, Farkasovsky M, Senohrabkova L, Vasicova P, Hasek J. New integrative modules for multicolor-protein labeling and live-cell imaging in Saccharomyces cerevisiae. *FEMS Yeast Res*. 2016;**16**:56.
32 Gonzalez A, Ruiz A, Serrano R, Arino J, Casamayor A. Transcriptional profiling of the protein phosphatase 2C family in yeast provides insights into the unique functional roles of Ptc1. *J Biol Chem*. 2006;**281**:35057–69.
33 Ferrando A, Kron SJ, Rios G, Fink GR, Serrano R. Regulation of cation transport in *Saccharomyces cerevisiae* the salt tolerance gene *HAL3*. *Mol Cell Biol*. 1995;**15**:5470–81.
34 Baggett J, Shaw J, Sciambi C, Watson H, Wendland B. Fluorescent labeling of yeast. *Curr Prot Cell Biol*. 2003;**20**:1–4.
35 Pelham HR. Evidence that luminal ER proteins are sorted from secreted proteins in a post-ER compartment. *EMBO J*. 1988;**7**:913–8.
36 Hurley JH. The ESCRT complexes. *Crit Rev Biochem Mol Biol*. 2010;**45**:463–87.
37 Olzhausen J, Moritz T, Neetz T, Schüller H-J. Molecular characterization of the heteromeric coenzyme A-synthesizing protein complex (CoA-SPC) in the yeast Saccharomyces cerevisiae. *FEMS Yeast Res*. 2013;**13**:565–73.
38 Laidlaw KME, MacDonald C. Endosomal trafficking of yeast membrane proteins. *Biochem Soc Trans*. 2018;**46**:1551–8.
39 Pavlin MR, Hurley JH. The ESCRTs – converging on mechanism. *J Cell Sci*. 2020;**133**:240333.
40 Jorgensen P, Rupes I, Sharom JR, Schneper L, Broach JR, Tyers M. A dynamic transcriptional network communicates growth potential to ribosome synthesis and critical cell size. *Genes Dev*. 2004;**18**:2491–505.
41 Novarina D, Guerra P, Milias-Argeitis A. Vacuolar Localization via the N-terminal Domain of Sch9 is Required for TORC1-dependent phosphorylation and downstream signal transduction. *J Mol Biol*. 2021;**433**:167326.
42 Chang T, Schroder LA, Thomson JM, Klocman AS, Tomasini AJ, Strømhaug PE, et al. PpATG9 encodes a novel membrane protein that traffics to vacuolar membranes, which sequester peroxisomes during pexophagy in Pichia pastoris. *Mol Biol Cell*. 2005;**16**:4941–53.
43 Brachmann CB, Davies A, Cost GJ, Caputo E, Li J, Hieter P, et al. Designer deletion strains derived from *Saccharomyces cerevisiae* S288C: a useful set of strains and plasmids for PCR-mediated gene disruption and other applications. *Yeast*. 1998;**14**:115–32.

Supporting information

Additional supporting information may be found online in the Supporting Information section at the end of the article.

Fig. S1. Characterization of strain MAC003, overexpressing a chromosomally encoded GFP-tagged version of Ppz1.

Table S1. Oligonucleotides employed in this work.